Treg-Related Genes Representing a Potential Shared Biological Mechanism Between Clear Cell Renal Carcinoma and Obesity

Xiaoqing Zhou, Peng Li, Qiangqiang Xu and Junjie Ye

Department of Urology, Postgraduate Training Base Alliance of Wenzhou Medical University, Lishui City People's Hospital, Lishui, China

ABSTRACT

Objective: To determine the potential shared biological mechanism between obesity and clear cell renal carcinoma (ccRCC).

Study Design: Observational study.

Place and Duration of the Study: Department of Urology, Lishui People's Hospital, Lishui City, China, from December 2022 to March 2023.

Methodology: The test and validation cohorts were selected from the GEO database. WGCNA and PPI networks were applied to identify shared hub genes. GO/KEGG, GSEA, and ROC curve analyses were applied to explore the potential underlying mechanisms and diagnostic power. Logistic regression was used to select genes to construct the signature. The risk score and various immune-related analyses were performed to assess the clinical and immune performance of the signature. The CellMiner platform was used to screen potential FDA-approved drugs.

Results: *PTPRC*, *TYROBP*, *ITGB2*, *CD86*, and *ITGAM* were defined as shared hub genes with good diagnostic power for obesity and ccRCC. Eight immune cells exhibited a positive correlation with the hub genes, while two immune cells showed negative associations. MDSCs and Tregs had the strongest positive associations with the hub genes. The Treg-related pathway exhibited predominant enrichment. The *TYROBP*, *ITGB2*, and *CD86* genes were selected to construct an immune signature that has good clinical and immune performance. Six FDA-approved drugs were screened.

Conclusion: Five Treg-related genes were identified as shared hub genes in obese patients and ccRCC patients. A signature was constructed to describe the immune features of ccRCC.

Key Words: *Treg-related genes, Shared biological mechanism, Immune signature, Obesity, Clear cell renal carcinoma (ccRCC)*.

How to cite this article: Zhou X, Li P, Xu Q, Ye J. Treg-Related Genes Representing a Potential Shared Biological Mechanism Between Clear Cell Renal Carcinoma and Obesity. *J Coll Physicians Surg Pak* 2024; **34(02)**:193-201.

INTRODUCTION

Renal cancer (RCC) is a prevalent urological malignancy that caused approximately 430,000 new cases and 180,000 deaths globally in 2020.[1] Currently, RCC accounts for 2% of global cancer diagnoses and deaths, and the incidence has more than doubled in the past half-century.[2] Clear cell renal carcinoma (ccRCC) is the main subtype of RCC and a main cause of tumour-associated death. In addition to race and specific genetic factors, such as von Hippel-Lindau disease, potential risk factors, including obesity, smoking, chronic kidney disease, and hypertension, have been identified.[3-5] These risk factors are often modifiable. Therefore, gaining a deeper understanding of these modifiable risk factors and their potential molecular mechanisms may provide a foundation for more precise preventive strategies and improvements in early diagnosis and treatment.

Correspondence to: Dr. Junjie Ye, Department of Urology, Postgraduate Training Base Alliance of Wenzhou Medical University, Lishui City People's Hospital, Lishui, China
E-mail: 905940344@qq.com

Received: May 30, 2023; Revised: December 29, 2023; Accepted: January 22, 2024
DOI: https://doi.org/10.29271/jcpsp.2024.02.193

Among the modifiable risk factors mentioned above, obesity is an independent risk factor and is concurrently associated with lipid accumulation in the proximal tubules, which serve as the origin site for ccRCC.[3,6] However, the relationship between obesity and RCC is intricate, and paradoxical aspects exist. The risk of developing RCC is 1.82 times greater in individuals with obesity than in those with normal body weight. On the other hand, the overall survival (OS) of obese RCC patients is greater than that of nonobese individuals.[1] Recently, research has been conducted to elucidate the association between circulating obesity-driven biomarkers and the risk of ccRCC, providing evidence for the relevance of insulin-resistance and chronic inflammation to ccRCC risk.[7] Therefore, exploring common biomarkers may offer novel directions for understanding the intricate relationship between obesity and RCC. In this study, the potential shared pathogenic mechanisms between RCC and obesity were investigated, and molecular signatures predicting the prognosis of RCC were constructed based on these common pathogenic markers. The objective of this study was to determine the potential shared biological mechanism between obesity and ccRCC.

METHODOLOGY

The ccRCC and obesity datasets were searched in the Gene Expression Omnibus (GEO) database (http://www.ncbi.nlm.nih.gov/geo/) with the criteria met; datasets should contain patient and control data, each group should include more than 20 samples, obesity/nonobesity samples should be derived from adipose tissues, ccRCC and normal samples should be derived from tumour and adjacent normal tissues, and samples from the validation cohort should be paired.

Data normalisation of the GEO datasets was performed using the "normalizeBetweenArrays" function of the limma R package. The WGCNA package in R was applied to construct coexpression networks, generate module eigengenes (MEs), and measure the association between MEs and the occurrence of disease with soft powers β set at 2 in obese patients and 11 in ccRCC patients. The other parameters were set as follows: minModuleSize = 50, mergeCutHeight = 0.25, TOMType = unsigned, and deepSplit = 2.

The gene coexpression module with the strongest positive correlation coefficient was extracted from the WGCNA results for obese patients and ccRCC patients. The common genes were identified as genes common to both obesity and ccRCC. Gene Ontology (GO) and Kyoto Encyclopedia of Genes and Genomes (KEGG) enrichment analyses were further performed to determine the potential biological functions of the genes using the clusterProfiler package in R. The cut-off value was set at $p<0.05$.

STRING (http://string-db.org) and Cytoscape (http://cytoscape.org/) were used to create the PPI networks. To further screen the core shared genes, the CytoHubaa and MCODE plugins were used. MCODE was used to screen the largest cluster with default parameters, and four algorithms in cytoHubba (Degree, EPC MCC, and MNC) were used to identify the top 10 genes. The common genes were defined as shared hub genes.

The ggpubr R package was used to determine the differential expression of common hub genes in the validation cohort. A significance threshold of $p<0.5$ was applied.

To evaluate the predictive power of the shared hub genes in ccRCC and obesity, ROC curves were generated, and AUC values were calculated by the pROC package in R in both the test and validation cohorts.

ssGSEA was used to measure the infiltration degrees of 28 types of immune cells in ccRCC and obesity patients by the GSVA package in R. The association between shared hub genes and immune cells was assessed using the ggcorrplot package in R. The reference gene sets of 28 immune cells were downloaded from TISIDB (http://cis.hku.hk/TISIDB/data/download/CellReports.txt). Cluster analyses of the ccRCC and obesity datasets were performed according to the infiltration status of immune cells. The correlation between shared hub genes and immune cells was calculated further, and the p-value was set at $p<0.01$.

GSEA was also conducted with GSEA software to compare the high-expression and low-expression groups according to the median expression of the hub shared genes. The significant cut-off values were set as follows: nominal p-values of <0.05, |normalized enrichment scores (NES)| >1 and false-positive rate (FDR) q values of <0.25.

A signature was constructed to guild clinical practice and describe immune characteristics. A multivariate logistic method was applied to select factors from the hub genes and obtain odds ratio OR values. The ORs were considered as the coefficients of the factors in the signature. Thus, the signature score was calculated as follows: $\sum$(gene expression × coefficient).

According to major clinical traits, the samples were divided into subgroups as follows: normal *vs*. ccRCC, I-II stage *vs*. III-IV stage, T1-T2 *vs*. T3-T4, M0 *vs*. M1, N0 *vs*. N1-N3, and G1-G4. The signature score of each subgroup was calculated. On the other hand, the samples were divided into high-risk groups and low-risk groups according to the median score. The immune infiltration, immune score, immune checkpoints expression, and HLA-related gene expression were analysed between the high- and low-risk groups.

The CellMiner database provides a description of 60 types of cancer cells and their response to FDA-approved drugs. It is a platform for screening potential drugs. The "NCI-60" profile was downloaded from the cellMiner platform (http://discover.nci.nih.gov/cellminer/loadDownload.do). Pearson analysis was used to calculate the correlation of the hub genes with the drugs. The two drugs with the minimum p-value were considered potential drugs.

RESULTS

According to the inclusion criteria, four GEO datasets were included. The GSE25401 (26 obese and 30 nonobese, GPL6244, Microarray) and GSE40435 (202 ccRCC and 202 controls, GPL10558, Microarray) datasets were screened as the discovery cohorts. The GSE92405 (24 obese and 24 nonobese, GPL19109, Microarray) and GSE53757 (72 ccRCC and 72 controls, GPL570, Microarray) datasets were considered the validation cohorts. Two paired twins (GSM2890455, GSM 2890456, GSM2890457, and GSM2890458) were excluded from GSE92405 because they had the same BMI category.

The GSE25401 and GSE40435 datasets were utilised for WGCNA. The cluster dendrograms of GSE40435 and GSE25401 are displayed in Figure 1, A and B. Seven modules were identified in the GSE40435 dataset (Figure 1C), and all seven modules were significantly different (green module: r=0.4, p=5e-09; red module: r=0.55, p=2e-17; blue module: r=0.5, p=3e-58; brown module: r=0.77, p=4e-41; turquoise module: r=-0.95, p=1e-99; yellow module: r=-0.17, p=0.02; grey module: r=-0.21, p=0.002). Nine modules were identified in the GSE25401 dataset (Figure 1D). The turquoise module (r=0.72, p=4e-10), black module (r=-0.36, p=0.006), and green module (r=-0.29, p=0.03) were associated with obesity. The two modules with the strongest positive correlation (blue module in GSE40435 and turquoise module in GSE25401). These two modules had 187 shared genes, which were selected for further analysis.

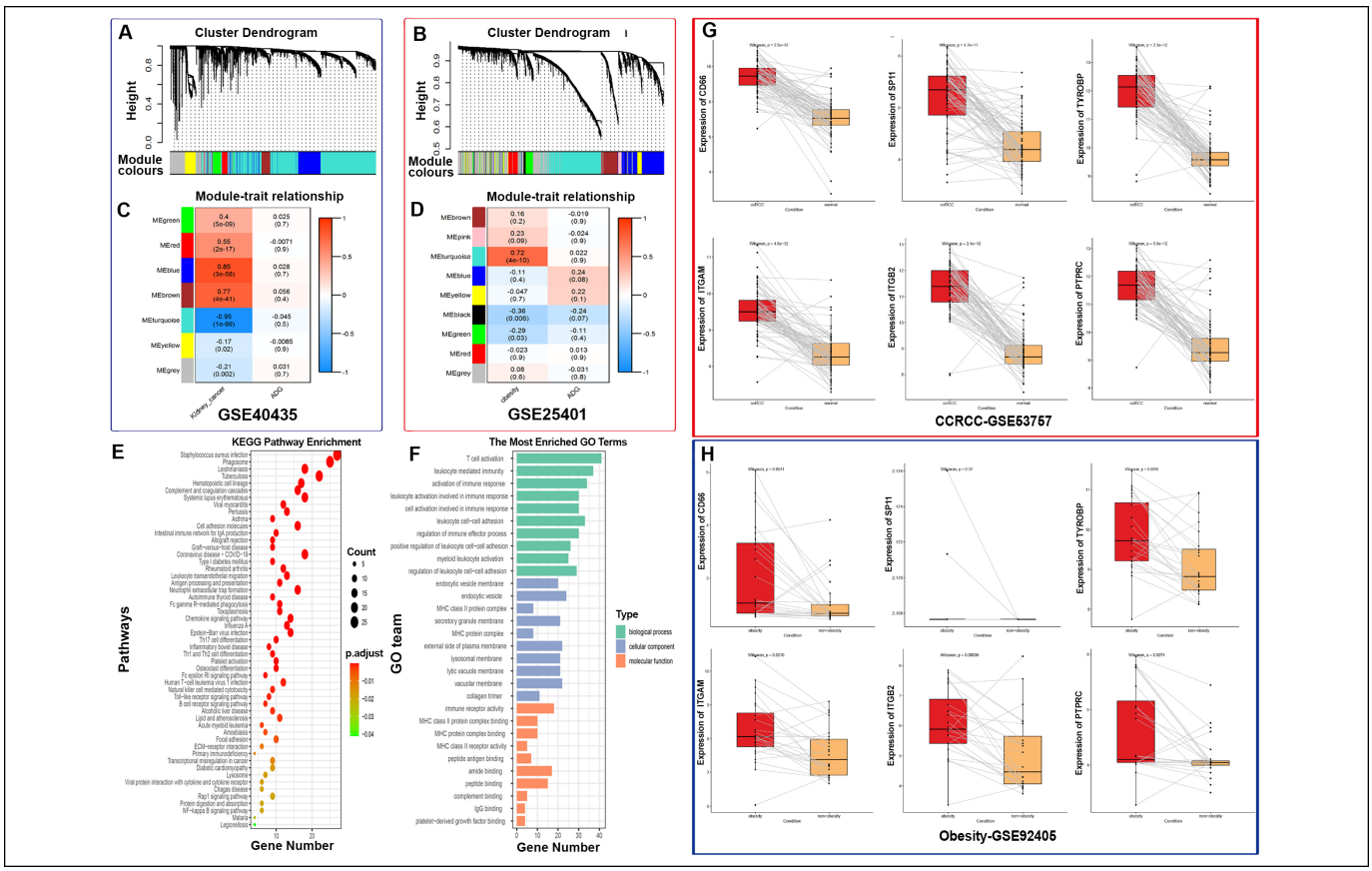

Figure 1: WGCNA, GO and KEGG enrichment analyses and the expression-verification of the hub genes. The cluster dendrogram of GSE40435 (A) and GSE25401 (B) The module-trait relationships of GSE40435 (C) and GSE25401 (D) The KEGG (E) and GO (F). Enrichment analysis of 187 overlapped genes of WGCNA. Six hub genes were more highly expressed in ccRCC tissues than normal tissues (G). Five hub genes were significantly more highly expressed in obese patients than in nonobese patients (H).

To interpret the potential biofunctions of the shared genes, GO and KEGG analyses were performed. The KEGG pathway enrichment data (Figure 1E) and the top 10 BP, CC, and MF terms (Figure 1F) are shown in Figure 1. Regarding molecular function and biological process terms, the shared genes were enriched in several terms involved in immune mechanisms (Figure 1F) as T-cell activation; leukocyte-mediated immunity, activation of immune response and immune receptor activity, and MHC class II protein complex binding. Furthermore, KEGG analysis showed that immunity may be involved in the shared mechanisms of tumours and obesity. The enriched pathways were as follows: intestinal immune network for IgA production, antigen processing and presentation, neutrophil extracellular trap formation, and Th17 cell differentiation (Figure 1E).

STRING and Cytoscape were used to further select hub genes. Four algorithms (Degree, EPC, MCC, and MNC) of cytoHubba were used to screen the top 10 genes. MCODE identified the largest cluster, which included 38 genes with an MCODE score = 31.676. There were six overlapping genes *PTPRC*, *TYROBP*, *SPI1*, *ITGB2*, *CD86*, and *ITGAM* in the five clusters.

The GSE92405 and GSE53757 datasets were utilised to validate the expression of shared hub genes. The box plot showed that *PTPRC*, *TYROBP*, *ITGB2*, *CD86*, and *ITGAM* were more highly expressed in ccRCC (Figure 1G) and obese patients (Figure 1H). *SPI1* was more highly expressed in ccRCC patients, with a p-value=4.7e-11 (Figure 1G). However, *SPI1* was not differentially expressed between obese and nonobese patients (Figure 1H).

The ROC curves illustrated the ability of the shared hub genes to predict ccRCC and obesity. The five shared hub genes had excellent diagnostic functions in ccRCC, with AUC values ranging from 0.92-0.97 (Figure 2, A and B), as well as good diagnostic functions in obesity, with AUC values ranging from 0.70-0.86 (Figure 2, C and D).

According to the GO and KEGG analyses, immunity may be a shared mechanism between ccRCC and obesity. Therefore, assessment of immune infiltration was assessed (Figure 2, E-H). Five hub genes were positively correlated with activated CD4 T cells, gamma delta T cells, regulatory T cells, myeloid-derived suppressor cells, and macrophages in both the ccRCC and obese groups (Figure 2, E and G). On the other hand, they were negatively correlated with T helper 17 cells, CD56 bright natural killer cells, and plasmacytoid dendritic cells in both the ccRCC and obese groups (Figure 2, E and G).

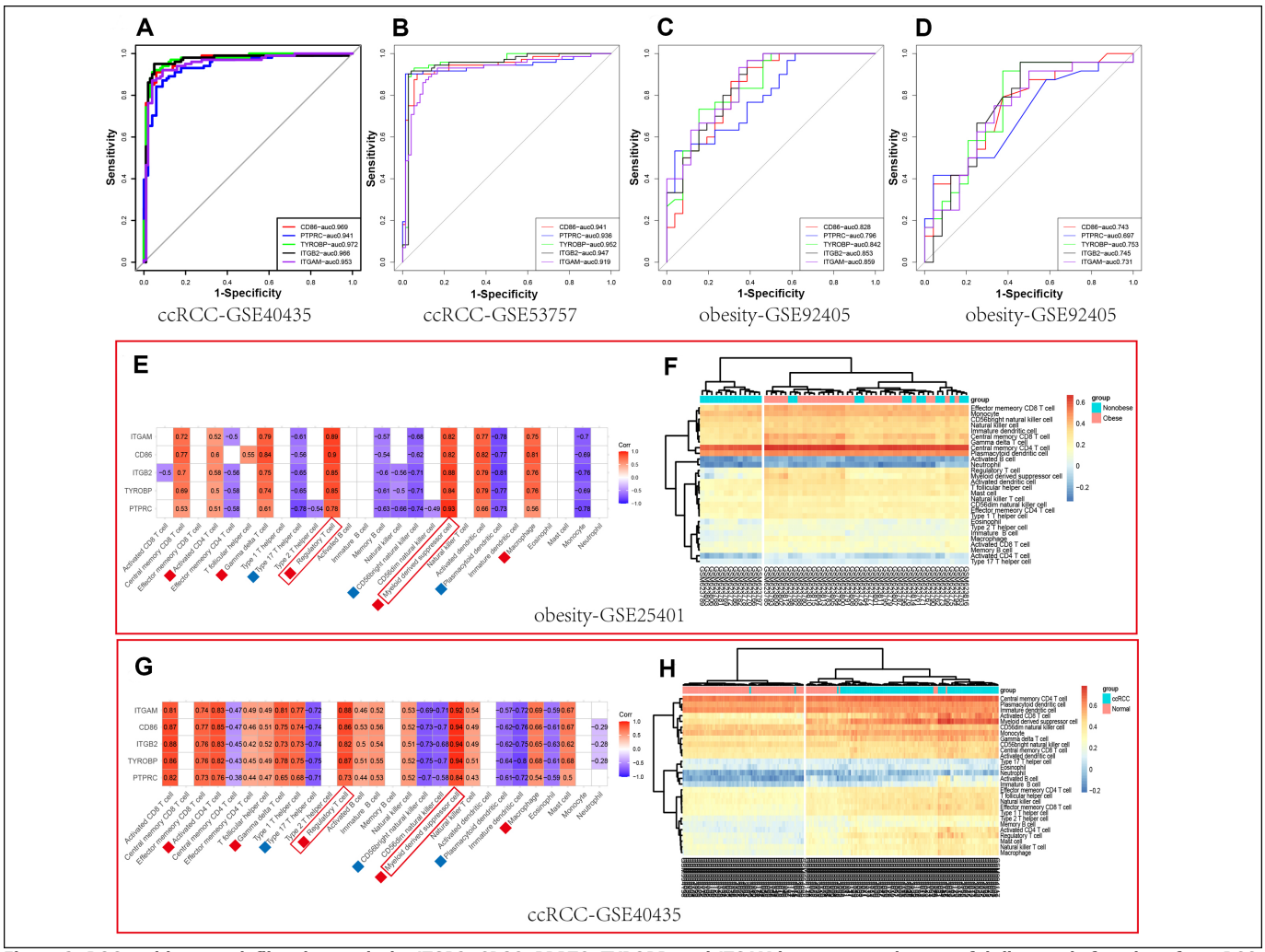

Figure 2: ROC and immune infiltration analysis. *ITGB2, CD86*, *PRPTC*, *TYROBP*, and *ITGAM* have extremely powerful diagnostic functions for ccRCC, with AUCs ranging from 0.92-0.97 (A-B), and highly powerful diagnostic functions for obesity with AUCs ranging from 0.70-0.86 (C-D). The immune cells marked with a red/blue block are positively/negatively correlated with the hub genes shared by obese patients (E). ssGSEA revealed that the immune statuses of "obese vs. nonobese" individuals were generally different (F). The same results were found in the ccRCC cohort (G, H). A "regulatory T-cell" and "myeloid-derived suppressor cell" marked with a red rectangle indicate that they were strongly positively associated with the hub genes in ccRCC patients and obese individuals.

Among the hub genes, myeloid-derived suppressor cells, and regulatory T cell, had the strongest positive associations. In general, the analysis of immune infiltration showed that ccRCC patients *vs*. normal individuals and obese patients *vs*. Nonobese patients had different immune statuses (Figure 2, F and H).

The GSE40435 and GSE25401 datasets were subjected to GSEA. The results revealed high expression of *ITGB2*, *CD86*, *PRPTC*, *TRYOBP*, and *ITGAM*, which were enriched mainly in the GOBP REGULATION OF REGULATORY T CELL DIFFERENTIATION and GOBP REGULATORY T CELL DIFFERENTIATION (Table I). This result was consistent with the immune infiltration data, which demonstrated that Treg cells were strongly correlated with the five hub genes.

CD86, *TYROBP*, and *ITGB2* were screened using multivariate logistic regression (Table II). Logistic regression was performed to determine the ORs (*CD86*-0.5758, *TYROBP*-1.0144, and *ITGB2*-0.9509) (Table II). Thus, the signature score was calculated as *CD86**0.57 +*TYROBP**1.01+*ITGB2** 0.95.

The risk scores of the clinical subgroups were calculated. The violin plots showed that the ccRCC group had a higher risk score than that the normal group (Figure 3A). The risk scores were greater in the advanced subgroups (T3-T4 group, N1-N3 group, M1 group, III-IV group, and G3-G4 group) than in the early-stage subgroup (Figure 3, B-D). This result indicated that the signature was strongly correlated with clinical traits and had a potential predictive power. The infiltration of 22 types of immune cells increased in the high-risk group (Figure 3E). The stomal score, immune score and ESTIMATE score of the high-risk group were greater than those of the low-risk group (Figure 3F). Most immune checkpoint genes (Figure 3G) and HLA-related genes were highly expressed in the high-risk group (Figure 3H).

Two potential FDA-approved drugs were screened for *CD86* (isotretinoin, R=0.75, p<0.001; megestrol acetate, R=0.7, p<0.001), *TYROBP* (artemether, R=0.73, p<0.001; imexon, R=0.63, p<0.001), and *ITGB2* (nelarabine, R=0.72, p<0.001; zalcitabine, R=0.7, p<0.001).

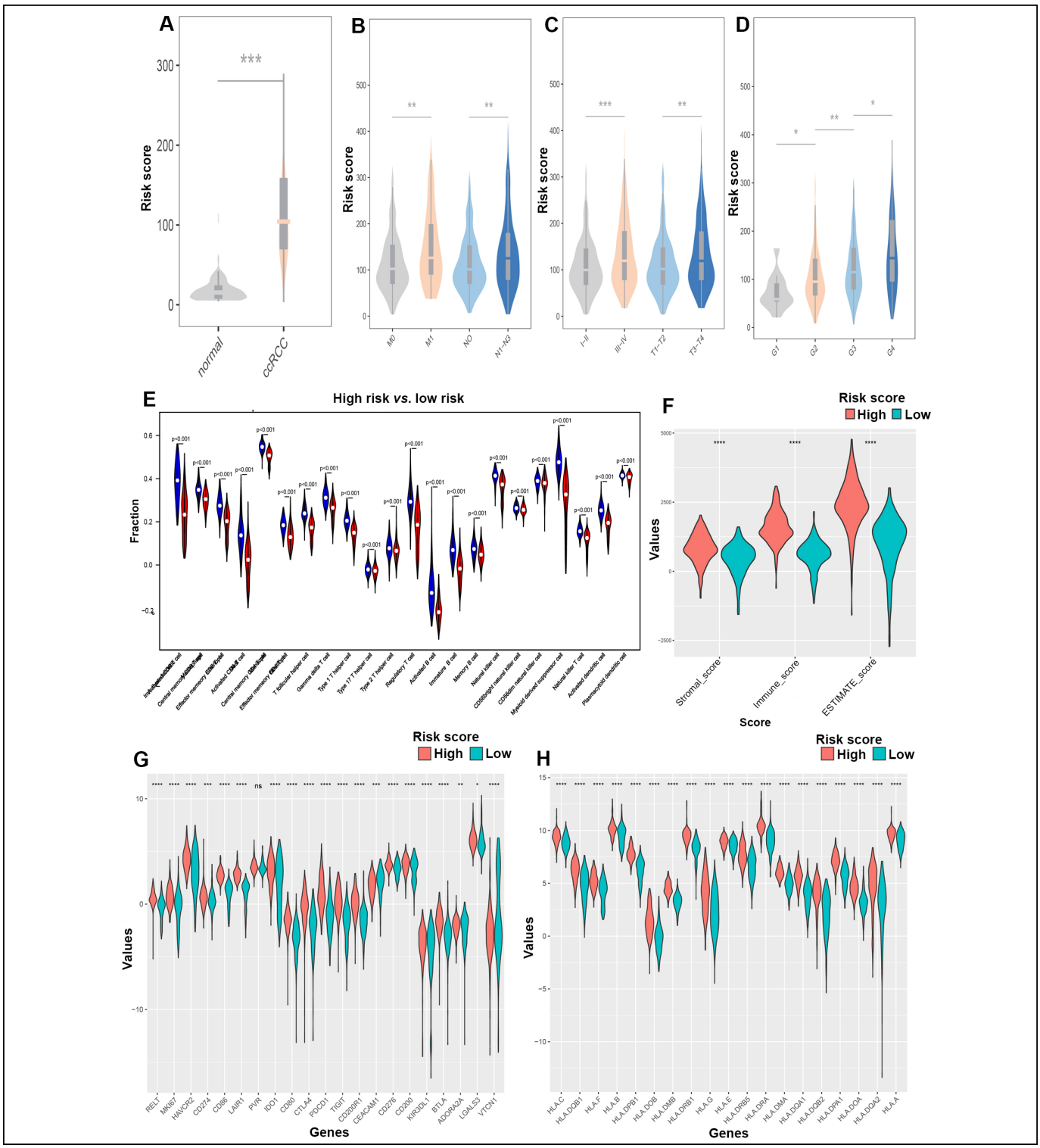

Figure 3: The risk score of clinical subgroups and the immune performance of the signature. The violin plots show that the ccRCC group had a high risk score (A). The advanced subgroup had higher risk scores (B-D). The relationship between the signature score and immune infiltration. There was differential infiltration of 22 types of immune cells between the high-risk group and low-risk group (E). Violin plots showing that the high-score group had higher stromal, immune and estimate scores (F). The violin plots showed that the high-score group had greater expression of immune checkpoint genes and HLA-related genes (G, H).

Table I: High expression of *ITGB2*, *CD86*, *PRPTC*, *TRYOBP*, and *ITGAM* in the GSE40435 (ccRCC) and GSE25401 (obesity) cohorts were all enriched in the GOBP REGULATION OF REGULATORY T CELL DIFFERENTIATION and GOBP REGULATORY T CELL DIFFERENTIATION.

GeneSet	Disease-genes	Enrichment Score (ES)	Normalised ES (NES)	Nominal p-value	FDR q-value
GOBP positive regulation of regulatory T-cell differentiation	ccRCC-*CD86*	0.86	1.71	0.00	0.01
	ccRCC-*ITGAM*	0.85	1.51	0.00	0.06
	ccRCC-*ITGB2*	0.86	1.52	0.00	0.12
	ccRCC-*PRPTC*	0.86	1.84	0.00	0.00
	ccRCC-*TYROBP*	0.86	1.62	0.00	0.04
	obesity-*CD86*	0.75	1.66	0.00	0.02
	obesity-*ITGAM*	0.77	1.95	0.00	0.00
	obesity-*ITGB2*	0.77	1.63	0.00	0.05
	obesity-*PRPTC*	0.77	1.96	0.00	0.01
	obesity-*TYROBP*	0.71	1.52	0.00	0.06
GOBP regulatory T-cell differentiation	ccRCC-*CD86*	0.82	1.73	0.00	0.01
	ccRCC-*ITGAM*	0.82	1.58	0.00	0.05
	ccRCC-*ITGB2*	0.81	1.52	0.00	0.12
	ccRCC-*PRPTC*	0.82	1.95	0.00	0.00
	ccRCC-*TYROBP*	0.81	1.67	0.00	0.03
	obesity-*CD86*	0.69	1.64	0.00	0.02
	obesity-*ITGAM*	0.71	1.97	0.00	0.00
	obesity-*ITGB2*	0.73	1.66	0.00	0.04
	obesity-*PRPTC*	0.71	1.97	0.00	0.00
	obesity-*TYROBP*	0.69	1.50	0.00	0.07

Table II: Multivariate logistic regression of five genes. The forest plot shows that *CD86*, *TYROBP*, and *ITGAM* were independent predictive factors. The three genes above were subjected to multivariate logistic regression analysis to determine the odds ratios (ORs) (*CD86*-0.5758, *TYROBP*-1.0144, and *ITGB2*-0.9509).

Multivariate logistics to screen genes			Multivariate logistics to obtain OR value	
Genes	**p-value**	**OR**	**p-value**	**OR**
CD86	4.09E-07	0.61 (0.50-0.73)	1.48E-12	0.57 (0.49-0.66)
PIPRC	0.2691	0.96 (0.90-1.02)		
TYROBP	0.00057	1.01 (1.00-1.01)	1.21E-05	1.01 (1.01-1.02)
ITGB2	0.00808	0.95 (0.92-0.98)	0.00078	0.95 (0.92-0.97)
ITGAM	0.44966	0.99 (0.96-1.02)		

DISCUSSION

Multiple previous epidemiologic surveys have indicated that obesity is a risk factor for kidney cancer and can facilitate tumour progression and metastasis.[6] Moreover, recent studies with big data have further confirmed these associations.[7] Several mechanisms have been explained. For example, the accumulation of adipose cells induces chronic hypoxia, increases tissue inflammation, and promotes insulin resistance, which provides an optimal microenvironment for tumour cells.[8] In addition, adipose tissue secretes adipokines and adiponectin, which stimulate carcinogenesis.[10]

In the present study, 187 common genes related to obesity and ccRCC were screened through WGCNA. Moreover, six genes were further selected by combining five types of algorithms. *PTPRC*, *TYROBP*, *ITGB2*, *CD86*, and *ITGAM*, which were significantly upregulated in both obese patients and ccRCC patients in the validation cohort, were defined as shared hub genes. In addition, ROC analysis revealed that *PTPRC*, *TYROBP*, *ITGB2*, *CD86*, and *ITGAM* had good diagnostic power for obesity and ccRCC with AUC values ranging from 0.92-0.97 and 0.70-0.86, respectively.

GO and KEGG analyses revealed that multiple pathways involving immunity, such as pathways related to T-cell activation, were significantly enriched. T-cell activation is a crucial component of the tumour immune mechanism and is highly dependent on the functionality of dendritic cells (DCs).[9] In addition, the transition between the quiescent and activated states of T-cells is influenced by various factors, such as the innate immune system, intracellular metabolic characteristics, and extracellular factors such as nutrients and regulatory T-cells, all of which can directly or indirectly impact this process.[10] Improving the understanding of T-cell activation pathways may provide opportunities to enhance the efficacy of immune checkpoint inhibitors and other immunotherapies. Correlation analysis revealed that eight types of immune cells had positive associations and that two types of immune cells had negative associations with five shared hub genes in both obese patients and ccRCC patients. These results indicated that immunological mechanisms may play an important role in the occurrence and development of obesity and ccRCC. According to the correlation analysis, myeloid-derived suppressor cells (MDSCs), and regulatory T-cells (Tregs) had the highest correlation coefficients with the hub genes. MDSCs are a group of heterogeneous cells composed of

bone marrow progenitor cells and immature myeloid cells (IMCs). MDSCs are involved in multiple aspects of immune regulation, such as cancer, inflammation, trauma, and graft-versus-host disease.[11] Tregs can suppress the function of effector T-cells and maintain immune system homeostasis.[12] In terms of immune function, MDSCs and Tregs were all classified as suppressive immune cells.[13] When the tumour microenvironment (TME) abnormally recruits MDSCs and Tregs, they establish an immunosuppressive TME together. On the other hand, Tregs can also recruit MDSCs to the TME to promote tumour escape.[14] In addition, the GSEA results indicated that the hub genes were highly enriched in Treg-related pathways (POSITIVE_REGULATION_OF_REGULATORY_T_CELL_DIFFERENTIATION and REGULATORY_T_CELL_DIFFERENTIATION). Thus, recruiting Tregs to acquire an immunosuppressive phenotype may be a common mechanism in ccRCC and obesity.

With advancements in research, the functions of tumour-infiltrating Treg cells is gradually being understood. Research on Tregs has progressed from identification to Treg-based therapies.[15] Tregs depletion has become a promising approach for suppressing antitumour immunity.[15] Furthermore, several studies have demonstrated that Treg depletion cannot only suppress tumours but also can enhance the efficacy of cancer vaccines.[16]

The identified hub genes strongly correlated with Tregs. To further explore the potential immune value of the hub genes, three hub genes were selected to construct a signature using multivariate logistic regression. To evaluate the value of the signature, comprehensive analysis was performed. The results showed that different subgroups of patients with different clinical traits had different risk scores. Moreover, immune infiltration and immune scores were different between the high-risk group and low-risk group. These results indicated that the signature can distinguish different clinical traits and immune situations.

Immunotherapy has been a powerful clinical treatment for cancer. Numerous immunotherapy drugs have been approved for clinical and preclinical treatment. Among them, immune checkpoint inhibitors (ICIs) constitute a major category. An increasing number of studies have demonstrated the efficacy of ICIs for solid malignancies.[17] On the other hand, HLA-related genes are critical for a variety of diseases, such as malignancies and infectious diseases.[18] In terms of ICIs, the biological influences of several HLA-related genes (such as *HLA-I*, *HLA-E*, *HLA-G*, and *HLA-A*) have been extensively confirmed in cancers.[19] Several HLA-related genes are considered as promising targets for solid cancer immuno-therapy.[20] Additionanlly, several clinical trials involving "anti-HLA" strategies have been launched.[21] In the present study, the expression of immune checkpoints genes and HLA-related genes was analysed between high-risk group and the low-risk group. The results showed that HLA-related genes and immune checkpoint genes (except for those related to *PVR*) were more highly expressed in high-risk group. However, datasets for estimating the ability of the signature to predict the efficacy of anti-PD1/HLA immunotherapy were unavailable. Finally, to improve the interpretability and clinical translation potential of the research, six potential FDA-approved drugs were screened using the CellMiner platform.

The five shared genes identified in this study and some of the results are consistent with previous research. For instance, Li *et al*. identified and validated *TYROBP* and *CD86*, which are more highly expressed in renal cancer tissues, using RT-qPCR.[22] Wu *et al*. screened *TYROBP* as a prognostic marker for renal cancer through immunohistochemistry (IHC) and validated its increased expression in renal cancer.[23] Naghdibadi *et al.* also reported that multiple genes, including *PTPRC* and *ITGAM*, are associated with immune infiltration in renal cancer.[24] Additionally, researchers constructed a RCC circulating tumour cell (CTCs) model, detected DEGs between CTCs and ccRCC tissues, and identified and validated two key genes, *TYROBP*, suggesting that these genes may influence CTC survival by regulating the tumour immune microenvironment.[25]

This study has several limitations. First, it was a bioinformatics analysis, and *in vitro* and *in vivo* experiments should be performed to verify the shared mechanism involved. Second, the present analysis was only at the transcriptional level, and data at the DNA and protein levels should be further collected to validate these conclusions.

CONCLUSION

PTPRC, *TYROBP*, *ITGB2*, *CD86*, and *ITGAM* were identified as shared hub genes in obesity and ccRCC. High infiltration of Tregs resulting in an immunosuppressive phenotype may act as a common mechanism underlying obesity and ccRCC. The *TYROBP*, *ITGB2*, and *CD86* genes were selected to construct an immune signature that has a good clinical and immune performance in ccRCC patients.

FUNDING:
This research was supported by the Lishui Welfare Technology Application Research Project (NO.2023GYX60/ NO.2019SJZC46/NO.2020GYX22); Zhejiang Medical Association Clinical Research Fund Project (No. 2022ZYC-A107).

ETHICAL APPROVAL:
This study was approved by the ethics committee of Lishui City People's Hospital (Approval No. LLW-FO-403).

PATIENTS' CONSENT:
Not applicable

COMPETING INTEREST

No conflicts of interest existed in this study.

AUTHORS' CONTRIBUTION:

JY: Research protocol design.
QX: Data collection.
XZ: Manuscript writing.
PL: Data analysis.
All authors reviewed the manuscript and consented to its publication.

REFERENCES

1. Yang J, Wang K, Yang Z. Treatment strategies for clear cell renal cell carcinoma: Past, present and future. *Front Oncol* 2023; **13**:1133832. doi:10.3389/fonc.2023.1133832.
2. Bukavina L, Bensalah K, Bray F, Carlo M, Challacombe B. Epidemiology of renal cell carcinoma: 2022 Update. *Eur Urol* 2022; **82**:529-42. doi:10.1016/j.eururo.2022.08.019.
3. Powell-Wiley TM, Poirier P, Burke LE, Despres JP, Gordon-Larsen P, *et al*. Obesity and cardiovascular disease: A scientific statement from the American Heart Association. *Circulation* 2021; **143**:e984-e1010. doi:10.1161/-CIR.0000000 000000973.
4. Bobulescu IA, Pop LM, Mani C, Turner K, Rivera C, Khatoon S, *et al*. Renal lipid metabolism abnormalities in obesity and clear cell renal cell carcinoma. *Metabolites* 2021;**11**. doi:10.3390/metabo11090608.
5. Wang Q, Tu H, Zhu M, Liang D, Ye Y, Chang DW, *et al*. Circulating obesity-driven biomarkers are associated with risk of clear cell renal cell carcinoma: A two-stage, case--control study. *Carcinogenesis* 2019; **40**:1191-7. doi:10.1093/carcin/bgz074.
6. Chow WH, Dong LM, Devesa SS. Epidemiology and risk factors for kidney cancer. *Nat Rev Urol* 2010; **7**:245-57. doi:10.1038/nrurol.2010.46.
7. Nam GE, Cho KH, Han K, Kim CM, Han B, Cho SJ, *et al.* Obesity, abdominal obesity and subsequent risk of kidney cancer: a cohort study of 23.3 million East Asians. *Br J Cancer* 2019; **121**:271-7. doi:10.1038/s41416-019-0500-z.
8. Kern PA, Ranganathan S, Li C, Wood L, Ranganathan, G. Adipose tissue tumor necrosis factor and interleukin-6 expression in human obesity and insulin resistance. *Am J Physiol Endocrinol Metab* 2001; **280**:E745-751. doi:10.1152/ajpendo.2001.280.5.E745.
9. Saibil SD, Ohashi PS. Targeting T cell activation in immuno-oncology. *Curr Oncol* 2020; **27**:S98-S105. doi:10. 3747/co.27.5285.
10. Chapman NM, Boothby MR, Chi H. Metabolic coordination of T cell quiescence and activation. *Nat Rev Immunol* 2020; **20**:55-70. doi:10.1038/s41577-019-0203-y.
11. Gabrilovich DI. Myeloid-derived suppressor cells. *Cancer Immunol Res* 2017; **5**:3-8. doi:10.1158/2326-6066.CIR-16- 0297.
12. Volta V, Perez-Baos S, dela Parra C. Katsara, O. Ernlund, A. Dornbaum, S. *et al*. A DAP5/eIF3d alternate mRNA translation mechanism promotes differentiation and immune suppression by human regulatory T cells. *Nat Commun* 2021; **12**:6979. doi:10.1038/s41467-021-27087-w.
13. Rahma OE, Hodi FS, The intersection between tumor angiogenesis and immune suppression. *Clin Cancer Res* 2019; **25**:5449-57. doi:10.1158/1078-0432.CCR-18-1543.
14. Holmgaard RB, Zamarin D, Li Y, Gasmi B, Munn DH, Allison JP, *et al*. Tumor-Expressed IDO Recruits and Activates MDSCs in a Treg-Dependent Manner. *Cell Rep* 2015; **13**: 412-24. doi:10.1016/j.celrep.2015.08.077.
15. Goschl L, Scheinecker C, Bonelli M. Treg cells in autoimmunity: From identification to Treg-based therapies. *Semin Immunopathol* 2019; **41**:301-14. doi:10.1007/s00281-019-00741-8.
16. Pastille E, Bardini K, Fleissner D, Adamczyk A, Frede A, Wadwa M, *et al*. Transient ablation of regulatory T cells improves antitumor immunity in colitis-associated colon cancer. *Cancer Res* 2014; **74**:4258-69. doi:10.1158/0008-5472.CAN-13-3065.
17. Lam TC, Tsang KC, Choi HC, Lee VH, Lam KO, Chiang CL, *et al.* Combination atezolizumab, bevacizumab, pemetrexed and carboplatin for metastatic EGFR mutated NSCLC after TKI failure. *Lung Cancer* 2021; **159**:18-26. doi:10.1016/ j.lungcan.2021.07.004.
18. Yuan X, Zhao Q, Zhang Y, Xue, M. The role and mechanism of HLA complex group 11 in cancer. *Biomed Pharmacother* 2021; **143**:112210. doi:10.1016/j.biopha.2021.112210.
19. Chowell D, Morris LGT, Grigg CM, Weber JK, Samstein RM, *et al*. Patient HLA class I genotype influences cancer response to checkpoint blockade immunotherapy. *Science* 2018; **359**:582-7. doi:10.1126/science.aao4572.
20. Salome B, Sfakianos JP, Ranti D, Daza J, Bieber C, Charap A, *et al.* NKG2A and HLA-E define an alternative immune checkpoint axis in bladder cancer. *Cancer Cell* 2022; **40:**1027-43 e1029. doi:10.1016/j.ccell.2022.08.005.
21. Loffler MW, Gori S, Izzo F, Mayer-Mokler A, Ascierto PA, Konigsrainer A, *et al*. Phase I/II multicenter trial of a novel therapeutic cancer vaccine, HepaVac-101, for hepatocellular carcinoma. *Clin Cancer Re* 2022; **28**:2555-66. doi:10.1158/1078-0432.CCR-21-4424.
22. Li F, Jin Y, Pei X, Guo P, Dong K, Chong T. Bioinformatics analysis and verification of gene targets for renal clear cell carcinoma. *Comput Biol Chem* 2021; **92**:107453. doi:10.1016/j.compbiolchem.2021.107453.
23. Wu P, Xiang T, Wan, J, Lv R, Wu G. TYROBP is a potential prognostic biomarker of clear cell renal cell carcinoma. *FEBS Open Bio* 2020; **10**:2588-604. doi:10.1002/2211-5463.12993.

24. Naghdibadi M, Momeni M, Yavari P, Gholaminejad A, Roointan, A. Clear cell renal cell carcinoma: A comprehensive in silico study in searching for therapeutic targets. *Kidney Blood Press Res* 2023; **48**:135-50. doi:10.1159/000529861.

25. Guo L, An T, Zhou H, Wan Z, Huang Z, Chong T. MMP9 and TYROBP affect the survival of circulating tumor cells in clear cell renal cell carcinoma by adapting to tumor immune microenvironment. *Sci Rep* 2023; **13**:6982. doi:10.1038/s41598-023-34317-2.